A Generally Weighted Moving Average Signed-Rank Control Chart

N. Chakraborty[a], S. Chakraborti[a,b], S.W. Human[1a], N. Balakrishnan[c]

[a]Department of Statistics, University of Pretoria, Pretoria, Lynnwood Road, Hillcrest, South Africa, 0002

[b]Department of Information Systems, Statistics and Management Science, University of Alabama, Tuscaloosa, AL 35487, U.S.A.

[c]Department of Mathematics and Statistics, McMaster University, Hamilton, Ontario, Canada L8S 4K1

Abstract: The idea of process monitoring emerged so as to preserve and improve the quality of a manufacturing process. In this regard, control charts are widely accepted tools in the manufacturing sector for monitoring the quality of a process. However, a specific distributional assumption for any process is restrictive and often criticised. Distribution-free control charts are efficient alternatives when information on the process distribution is partially or completely unavailable. In this article, we propose a distribution-free generally weighted moving average (GWMA) control chart based on the Wilcoxon signed-rank (SR) statistic. Extensive simulation is done to study the performance of the proposed chart. The performance of the proposed chart is then compared to a number of existing control charts including the parametric GWMA chart for subgroup averages, a recently proposed GWMA chart based on the sign statistic and an exponentially weighted moving average (EWMA) chart based on the signed-rank statistic. The simulation results reveal that the proposed chart performs just as well and in many cases better than the existing charts, and therefore can serve as a useful alternative in practice.

Keywords: Control chart; Distribution-free; Average run-length; Generally weighted moving average; Signed-rank statistic,

1. Introduction

Control charts are known to be efficient tools for monitoring quality of products. In the present era of highly sophisticated technology, it is of increasing importance to design control charts that are efficient in detecting small shifts in the characteristics of interest in a production process. While the Shewhart-type charts are the best known and most widely used in practice due to their inherent simplicity and global performance, other classes of charts, such as the exponentially weighted moving average (EWMA) and the generally weighted moving average (GWMA) charts are useful and sometimes more naturally appropriate.

The traditional EWMA chart for the mean was introduced by Roberts[1] and includes the Shewhart-type chart as a special case. The literature on EWMA charts is vast and still continues to grow at a considerable pace. The reader is referred to the overview on EWMA charts by Ruggeri et al.[2] and the references therein. A generalization of the EWMA chart, referred to as the Generally Weighted Moving Average (GWMA) chart, was proposed by Sheu and Lin[3] and they showed that it does perform better in detecting small shifts in the process mean.

In typical applications of the GWMA chart, it is usually assumed that the underlying process distribution is normal. If normality is in doubt or cannot be justified, a distribution-free control chart is more desirable. For an overview on distribution-free control charts and their advantages, the reader is referred to Chakraborti et al.[4].

[1] Corresponding author: e-mail: schalk.human@up.ac.za

Amin and Searcy[5] proposed an EWMA chart based on the Wilcoxon signed-rank statistic (EWMA-SR chart) for monitoring the known value of the median of a process. Graham et al.[6] further studied the practical implementation and performance of the EWMA-SR chart. Graham et al.[7] proposed an EWMA chart based on the sign statistic (EWMA-SN chart). Lu[8] proposed the GWMA chart based on the sign statistic, called the GWMA sign (GWMA-SN) chart, and showed that it outperforms the EWMA-SN chart for small shifts and performs similarly for large shifts. Lu[8] also showed that the GWMA-SN chart is more efficient than the parametric GWMA chart for the mean (GWMA-$\overline{X}$ chart) for underlying normal and many non-normal distributions. It is therefore only natural to further investigate and develop the GWMA control chart based on some other (and more efficient) nonparametric or distribution-free statistics.

The Wilcoxon signed-rank (SR) test is a popular nonparametric alternative to the paired two-sample *t*-test, but has the advantage that normality is not needed; only symmetry of the underlying continuous process distribution is needed which is easy to verify (see Konijin[9] for a discussion on some tests of symmetry). Furthermore, it is well known that the SR test is more efficient than the sign (SN) test for a number of non-normal symmetric continuous distributions (see Gibbons and Chakraborti[10]. In addition, it can be shown that the Asymptotic Relative Efficiency (ARE) of the SR test relative to the Student *t*-test is at least 0.864 for any symmetric continuous distribution (see Gibbons and Chakraborti[10], page 508).

In this article, we propose a GWMA chart based on the Wilcoxon signed-rank statistic (hereafter referred to as the GWMA-SR chart) to monitor the known value of the median of a process with a continuous distribution; the objective is to gain better sensitivity for small sustained upward or downward step shifts. The median is taken as the location parameter of interest as it is more robust and therefore a better choice than the mean for measuring the central value. Moreover, the Wilcoxon signed-rank test considers the median as the location parameter of interest.

The rest of this article is organised as follows: The GWMA-SR chart is defined in Section 2. In Section 3, the design and implementation of the proposed control chart is provided. A detailed empirical study comparing the performance of the GWMA-SR chart with a number of existing control charts is provided in Section 4. An illustrative example is given in Section 5. Finally, a concluding summary and some recommendations are presented in Section 6.

2. GWMA signed-rank (GWMA-SR) control chart

Let X be the quality characteristic of interest and assume its underlying distribution to be continuous and symmetric around θ. We take θ to be the median as it is a more robust measure and a better representative of the central value of a distribution than the mean. Let θ_0 denote the known value of θ.

Suppose X_{ij}, where $i = 1,2,3,\ldots$ and $j = 1,2,\ldots,n$, denotes the j^{th} observation in the i^{th} random sample (or rational subgroup) of size $n > 1$. Let R_{ij}^{+} denote the ranks of the absolute differences $\left|X_{ij} - \theta_0\right|$, for $j = 1,2,\ldots,n$, within the i^{th} subgroup. Define the statistic

$$SR_i = \sum_{j=1}^{n} sign\left(X_{ij} - \theta_0\right) R_{ij}^{+}, \;\; i = 1,2,3,\ldots, \qquad (1)$$

where $sign(x) = +1$ or -1 if $x > 0$ or $x < 0$, respectively. Therefore, it is easily verified that $SR_i = T_i^+ - T_i^-$ is the difference between the sum of the ranks of the $|X_{ij} - \theta_0|$'s corresponding to positive and negative differences, respectively, within the i^{th} subgroup. Also, SR_i can be re-written as $SR_i = 2T_i^+ - \frac{n(n+1)}{2}$ because the sum of all the ranks within a sample $T_i^+ + T_i^- = \frac{n(n+1)}{2}$; this relationship between the statistics will be used later to show that the proposed GWMA control chart is non-parametric or distribution-free. Note that, as the random sample is assumed to be drawn from a continuous distribution, the probability of tied observations, i.e. $\Pr[X_{ij} = \theta_0]$, is theoretically zero and therefore ignored.

Let N be the discrete random variable denoting the number of samples until the next occurrence of an event since its last occurrence. Then, by summing over all possible time periods, we can write

$$\sum_{i=1}^{\infty} \Pr[N = i] = \sum_{i=1}^{t} \Pr[N = i] + \Pr[N > t] = 1. \quad (2)$$

A generally weighted moving average (GWMA) is a weighted moving average (WMA) of a sequence of SR_i statistics with the probability $\Pr[N = i]$ being regarded as the weight of the i^{th} most recent statistic SR_{t-i+1}. In other words, the probability $\Pr[N = 1]$ is the weight of the latest or most recent observation SR_t and the probability $\Pr[N = t]$ is the weight of the most out-dated or oldest observation SR_1. The probability $\Pr[N > t]$ is taken to be the weight of the starting value, denoted by Z_0, which is typically taken as the in-control (IC) expected value of the statistic under consideration, i.e. $Z_0 = E(SR_i|\text{IC}) = 0$. Therefore, the charting statistic for the GWMA-SR chart can be defined as

$$Z_t = \sum_{i=1}^{t} \Pr[N = i]\ SR_{t-i+1} + \Pr[N > t]\, Z_0 \quad \text{for} \quad t = 1,2,3,..., \quad (3)$$

where $Z_0 = E(SR_i|\text{IC}) = 0$ is the starting value of the chart. As in Sheu and Lin[3], the distribution of N is taken to be $\Pr[N = i] = q^{(i-1)^\alpha} - q^{i^\alpha}$, where $0 \le q < 1$ and $\alpha > 0$ are two parameters; this is the discrete two-parameter Weibull distribution (Nakagawa and Osaki[11]). By substituting $Z_0 = 0$ and the probability mass function (p.m.f.) of the two-parameter Weibull distribution in equation (3), the charting statistic for the GWMA-SR chart simplifies to

$$Z_t = \sum_{i=1}^{t} (q^{(i-1)^\alpha} - q^{i^\alpha})\ SR_{t-i+1} \quad \text{for} \quad t = 1,2,3,\dots . \quad (4)$$

Note that the GWMA-SR chart reduces to the EWMA-SR chart when $\alpha = 1$ and $q = 1 - \lambda$, where $0 < \lambda \le 1$ is the smoothing parameter of the EWMA chart. The EWMA-SR chart further reduces to the Shewhart-SR chart when $q = 0$ and $\alpha = 1$. The GWMA chart can therefore be viewed as a generalisation of both EWMA and Shewhart-type charts with an additional parameter α that provides more flexibility in designing the chart. The in-control (IC) expected value and variance of the charting statistic Z_t are given by

$$E(Z_t|\text{IC}) = \sum_{i=1}^{t} \left(q^{(i-1)^\alpha} - q^{i^\alpha}\right)\ E(SR_{t-i+1}) = 0 \quad (5)$$

and

$$\text{var}(Z_t|\text{IC}) = \sum_{i=1}^{t} \left(q^{(i-1)^\alpha} - q^{i^\alpha}\right)^2\ \text{var}(SR_{t-i+1}) = \frac{n(n+1)(2n+1)}{6} Q_t, \quad (6)$$

respectively, where $Q_t = \sum_{i=1}^{t} \left(q^{(i-1)^\alpha} - q^{i^\alpha}\right)^2$ is the sum of squares of the weights. Equations (5) and (6) are derived using the results in Gibbons and Chakraborti[10] (page 198) for the mean and variance of the well-known Wilcoxon signed-rank test statistic coupled with the properties of the EWMA charting statistic (see Montgomery[12], page 419).

The exact time-varying (and symmetrically placed) upper control limit (UCL_e), lower control limit (LCL_e) and centerline (CL_e) of the GWMA-SR chart are given by

$$UCL_e/LCL_e = \pm L\sqrt{\frac{n(n+1)(2n+1)}{6}Q_t} \quad \text{and} \quad CL_e = 0, \tag{7}$$

where $L > 0$ is the distance of the control limits from the centerline.

The asymptotic variance of the charting statistic Z_t is given by $\lim_{t\to\infty} \text{var}(Z_t|\text{IC}) = \frac{n(n+1)(2n+1)}{6}Q$, where $Q = \lim_{t\to\infty} Q_t$, which is an increasing function of t and converges as $t \to \infty$ (see the Appendix for more detail).

The steady-state control limits are used when the process has been running for several time periods and are based on the asymptotic variance of the charting statistic (see Lucas and Saccucci[13]). The steady-state control limits and the centerline are given by

$$UCL_s/LCL_s = \pm L\sqrt{\frac{n(n+1)(2n+1)}{6}Q} \quad \text{and} \quad CL_s = 0, \tag{8}$$

where the subscript "s" denotes the steady-state values.

The following points are worth noting:

i. The distribution of the SR_i statistic is discrete, symmetric about zero and its extreme values, i.e. the minimum and maximum, are $\frac{-n(n+1)}{2}$ and $\frac{n(n+1)}{2}$, respectively; these extremes occur when all the observations within a subgroup are less than or greater than θ_0, respectively;
ii. We study two-sided GWMA-SR charts with symmetrically placed control limits, i.e. equidistant from the centerline. The methodology can be easily modified wherein a one-sided chart is more meaningful or when two-sided control charts with asymmetric control limits are necessary;
iii. Steady-state control limits are used in order to simplify the application/implementation of the chart. For the sake of notational simplicity, we will use UCL and LCL hereafter to denote the steady-state control limits;
iv. If any charting statistic Z_t plots on or outside either of the control limits given by equation (8), a signal is given and the process is declared to be out-of-control (OOC). Otherwise, the process is considered to be in-control (IC), which implies that no location shift has occurred, and the charting procedure continues on.

In the next section, we discuss the design of the proposed GWMA-SR chart in more detail.

3. The design and implementation of GWMA-SR chart

Performance measures are needed to design and compare the performance of control charts. The traditional approach of evaluating a control chart is to obtain the run-length distribution and its associated characteristics. The run-length is a discrete random variable that represents the number of samples which must be collected (or, equivalently, the number of charting statistics that must be plotted) in order for the chart to detect a shift or give a signal. An intuitively appealing and popular measure of a chart's performance is the average run-length (ARL), which is the expected number of charting statistics that must be plotted in order for the chart to signal (see Human and Graham[14]). Clearly, for an efficient control chart, one would like to have the in-control ARL (denoted ARL_0) to be "large" and the out-of-control ARL (denoted ARL_1) to be "small". Although other measures such as the standard deviation of the run-length ($SDRL$) and various upper and lower percentiles could be and have been used to supplement the evaluation of control charts, the ARL is the most widely used measure due to its intuitive appealing interpretation. Therefore, we use here the ARL to design and compare the performance of the proposed GWMA-SR chart to other charts.

The design of a control chart typically involves solving for the combination of the chart's parameters, i.e. α, q and L, so as to obtain a pre-specified in-control average run-length denoted by ARL_0^*. The computational aspects of the run-length distribution for the GWMA-SR chart are discussed next, followed by the design of the GWMA-SR control chart.

3.1 The run-length distribution of the GWMA-SR chart

Suppose the run-length random variable is denoted by R and that A_i denotes the signalling event at the i^{th} sample. The complimentary event is the non-signalling event and is the event that there is no signal at the i^{th} sample, i.e. $A_i^c = [LCL < Z_i < UCL]$ for $i = 1,2,3,...$. Then, in general, the run-length distribution can be written as $\Pr[R = r] = \Pr[\{\cap_{i=1}^{r-1} A_i^c\} \cap A_r]$, for $r = 1,2,3,...$; i.e. there is a signal for the first time at the r^{th} sample. For any $i > 1$, we can re-write the event that a charting statistic is between the control limits, i.e. $A_i^c = [LCL < Z_i < UCL]$, as $A_i^c = [L_i < SR_i < U_i]$, where $U_1 = \frac{UCL}{1-q}$ and $L_1 = \frac{LCL}{1-q}$, respectively, and

$$U_i = \frac{UCL - \sum_{j=2}^{i}\left(q^{(j-1)^\alpha} - q^{j^\alpha}\right) SR_{i-j+1}}{1-q} \text{ and } L_i = \frac{LCL - \sum_{j=2}^{i}\left(q^{(j-1)^\alpha} - q^{j^\alpha}\right) SR_{i-j+1}}{1-q}, \text{ for } i = 2,3,4,\ldots \quad (9)$$

The benefit of re-writing the non-signalling event is as follows: Instead of working with the joint distribution of a sequence of dependent charting statistics, i.e. the Z_i's (which is compared to the steady-state control limits in equation (8)), one works with the joint distribution of a sequence of independent sample statistics SR_i (which is compared to the varying limits in (9)). The run-length distribution can therefore be written as

$$\Pr[R = 1] = 1 - \Pr[L_1 < SR_1 < U_1] \quad \text{and} \quad \Pr[R = r] = I_{r-1} - I_r\,, \quad (10)$$

where $I_r = \Pr[\cap_{i=1}^{r} A_i^c] = \Pr[\cap_{i=1}^{r} \{L_i < SR_i < U_i\}]$ for $r = 2,3,4,...$; see the Appendix for more detail.

As the samples are assumed to be independent, the SR_i's are independent and an expression for I_r can be obtained using the relationship $SR_i = 2T_i^+ - \frac{n(n+1)}{2}$; see Gibbons and Chakraborti[10] (page 198) for more detail on the statistic T_i^+. An expression for I_r is given by

$$I_r = \sum_{L_1}^{U_1} \sum_{L_2}^{U_2} \ldots \sum_{L_r}^{U_r} \left(\prod_{i=1}^{r} \Pr\left(T_i^+ = \frac{2s_i + n(n+1)}{4}\right)\right), \quad (11)$$

where $T_i^+ = \sum_{j=1}^{n} I(X_{ij} - \theta_0) R_{ij}^+$ with $I(x) = 1$ or 0 if $x > 0$ or $x < 0$, respectively, s_i denotes the observed value of the statistic SR_i, and n is the sample size. The ARL can also be expressed in terms of I_{r} as (see the Appendix for more detail)

$$ARL = 1 + \sum_{r=1}^{\infty} I_{\mathrm{r}} \ . \tag{12}$$

The following comments regarding equations (11) and (12) are essential:

i. Because the in-control distribution of T_{i}^+ does not depend on the underlying process distribution (see Gibbons and Chakraborti[10]), the run-length probabilities and the ARL_0, which are both functions of I_{r}, are the same for all continuous symmetric distributions. This makes the proposed GWMA-SR chart a distribution-free control chart;

ii. To analytically evaluate equations (11) and (12) is time-consuming and uneconomical for a number of reasons:

   a. The lower and upper bounds in the summations of I_{r}, i.e. U_{i} and L_{i} given in equation (9), are dependent and functions of the sequence of preceding statistics $SR_1, SR_2, \ldots, SR_{i-1}$; these bounds cannot be economically recursively updated and is therefore a computationally expensive approach;

   b. The number of terms in equation (11) that needs to be evaluated increases dramatically as r increases;

   c. The out-of-control distribution of the statistic T_{i}^+ is not known.

   Due to these difficulties, extensive simulation is used to calculate the ARL values for the proposed GWMA-SR chart. To this end, it is important to note that, Sheu and Lin[3], Sheu and Yang[15] and Lu[8] have also mentioned that the run-length distribution of the GWMA charts cannot be obtained by either the Markov chain approach or by the recursive integral equation approach.

3.2 Design of the GWMA-SR chart

For a given or chosen sample size n, the two parameters q and α are varied over a certain range and for each (q, α) combination, the values of the charting constant, i.e. $L > 0$, are obtained so that the attained in-control ARL is close to (in this case slightly above or below due to the use of simulation) the nominal or specified value ARL_0^*. We consider four sample sizes, i.e. $n =$ 5, 10, 15 and 20; one may consider other values of n too. The typical industry standards for ARL_0^* are 370 or 500 and we consider the former in our study. The typical recommendation for the smoothing parameter $0 < \lambda \leq 1$ for an EWMA chart is to choose smaller values for smaller shifts (see Montgomery[12], page 423). Because the GWMA chart reduces to an EWMA chart when $q = 1 - \lambda$ and $\alpha = 1$, a larger value of q, i.e. closer to 1, should be a reasonable choice for the GWMA chart to detect smaller shifts. To this end, Sheu and Lin[3] noted that (q, α) combinations in the intervals $0.5 \leq q \leq 0.9$ and $0.5 \leq \alpha < 1$ enhanced the sensitivity of the GWMA-$\bar{X}$ chart and outperformed the EWMA-$\bar{X}$ chart for small shifts (i.e. less than 1.5 standard deviations in the location). The same range of (q, α) values were also considered by Sheu and Yang[15], Teh et al.[16], Sheu et al.[17] and Lu[8]. In our simulation study, we considered the range $q = 0.5$ (0.1) 0.9 and the range $\alpha = 0.1$ (0.1) 1.5, which is slightly larger than those used in previous studies.

Using simulation together with a grid search algorithm, we obtained the charting constant $L > 0$ for the chosen (q, α) combination and specified sample size n, so that the attained ARL_0 is approximately equal to $ARL_0^* = 370$; the values of L thus determined are presented in Table 1 along with the attained ARL_0 values in parenthesis. The L values in Table 1 will be useful for the design and implementation of the GWMA-SR chart.

To ensure our simulation yields reasonable and consistent results, we compared our results to those obtained by Graham et al.[6]; this was possible for two reasons: (a) the GWMA-SR chart reduces to EWMA-SR chart when $q = 1 - \lambda$ and $\alpha = 1$, and (b) the EWMA-SR chart by Graham et al.[6] uses steady-state control limits. Consider, for example, the following two scenarios:

i. When n = 5, q = 0.8 and α = 1, we find from Table 1 that a value of $L = 2.768$ gives an attained $ARL_0 = 370.90$. In Graham et al.[6], the EWMA-SR chart with n = 5, $\lambda = 1 - q = 0.2$ and $L = 2.764$ has an attained $ARL_0 = 369.91$;
ii. When $n = 10$, $q = 0.9$ and $\alpha = 1$, we find from Table 1 that a value of $L = 2.683$ gives an attained $ARL_0 = 370.12$. In Graham et al.[6], the EWMA-SR chart with n = 10, $\lambda = 1 - q = 0.1$ and $L = 2.684$ has an attained ARL_0 = 370.09.

To further investigate the behaviour of the in-control ARL as a function of the parameters α, $q = 1 - \lambda$ and L, we calculated the attained ARL_0 for certain combinations of the parameters. We chose $n = 10$, $\alpha = 0.5(0.1)0.9$, $q = 0.5(0.1)0.9$ and set L =2.0, 2.5, 3.0 and 2.79; the latter value was chosen based on the values reported in Table 1. The obtained results are displayed in Figure 1. Note that the line graphs in each of the panels display the attained ARL_0 on the vertical axis versus the value of q on the horizontal axis for a certain combination of (α, L). The attained ARL_0 values are shown in the data tables below the graphs for ease of reference.

From Figure 1, we observe the following:

i. For $L = 2.0$ and 2.50 in panels (c) and (d), the attained ARL_0 is a monotonically increasing function of q;
ii. For L =2.79 and 3.0 in panels (a) and (b), the attained ARL_0 is a decreasing function of q when $0.5 \leq q \leq 0.8$ and thereafter increases. This implies that, in general, multiple combinations of the parameters (q, α, L) will yield the same ARL_0. This is somewhat problematic because, apart from desiring a sufficiently large ARL_0, the ARL_1 should be small for an effective GWMA-SR chart. Therefore, the (q, α, L) combination with the minimum ARL_1 for a specified shift δ is said to be the optimal combination. The optimal design of the GWMA-SR chart consists of specifying the desired ARL_0 and ARL_1 values and the magnitude of the process shift that is anticipated and then select the

Table 1: Values of L for the GWMA-SR charts for different (q, α) when n = 5(5)20 and $ARL_0^* = 370$

		q				
n	α	0.5	0.6	0.7	0.8	0.9
5	0.1	2.133 (370.32)	2.146 (368.28)	2.158 (371.61)	2.169 (369.91)	2.180 (370.93)
	0.2	2.234(371.50)	2.262 (373.71)	2.287 (371.16)	2.310 (368.37)	2.332 (366.31)
	0.3	2.320 (367.80)	2.363 (371.12)	2.402 (369.37)	2.439 (369.72)	2.470 (369.87)
	0.4	2.396 (372.61)	2.451 (370.30)	2.502 (369.96)	2.548 (367.92)	2.573 (371.58)
	0.5	2.458 (369.87)	2.523 (370.01)	2.583 (369.86)	2.631 (370.68)	2.631 (370.86)
	0.6	2.510 (370.69)	2.582 (369.81)	2.646 (370.38)	2.686 (369.55)	2.657 (369.88)
	0.7	2.553 (369.63)	2.628 (369.11)	2.688 (369.38)	2.724 (369.48)	2.667 (370.69)
	0.8	2.588 (370.29)	2.665 (370.61)	2.721 (370.72)	2.747 (370.28)	2.668 (370.01)
	0.9	2.615 (370.56)	2.690 (369.86)	2.742 (369.62)	2.761 (369.44)	2.667 (370.34)
	EWMA 1.0	2.638 (370.79)	2.708 (370.09)	2.757 (369.96)	2.768 (370.91)	2.666 (369.90)
	1.1	2.657 (372.24)	2.728 (367.20)	2.768 (373.80)	2.769 (369.40)	2.670 (369.76)
	1.2	2.670 (369.98)	2.733 (372.94)	2.767 (367.36)	2.767 (370.72)	2.671 (369.19)
	1.3	2.681 (371.19)	2.735 (367.96)	2.767 (368.47)	2.765 (370.19)	2.679 (371.02)
	1.4	2.689 (369.26)	2.739 (370.88)	2.765 (368.76)	2.758 (369.41)	2.685 (371.74)
	1.5	2.694 (368.95)	2.739 (369.19)	2.761 (370.30)	2.757 (370.94)	2.690 (370.48)
10	0.1	2.708 (369.80)	2.708 (375.07)	2.706 (372.49)	2.704 (370.07)	2.704 (371.35)
	0.2	2.707 (372.19)	2.709 (371.54)	2.714 (372.69)	2.716 (370.17)	2.717 (365.09)
	0.3	2.719 (368.82)	2.726 (368.38)	2.733 (368.20)	2.740 (371.50)	2.743 (371.98)
	0.4	2.734 (367.96)	2.747 (369.42)	2.760 (369.94)	2.767 (368.65)	2.757 (371.09)
	0.5	2.751 (369.86)	2.768 (369.96)	2.785 (370.59)	2.791 (370.32)	2.751 (370.29)
	0.6	2.768 (370.42)	2.790 (370.45)	2.807 (369.93)	2.804 (370.59)	2.735 (370.69)
	0.7	2.783 (370.32)	2.806 (369.98)	2.822 (370.15)	2.814 (370.34)	2.718 (370.48)
	0.8	2.797 (369.95)	2.822 (370.47)	2.832 (369.48)	2.816 (370.26)	2.698 (369.07)
	0.9	2.805 (369.89)	2.833 (369.39)	2.841 (370.87)	2.815 (369.34)	2.687 (370.88)
	EWMA 1.0	2.815 (370.78)	2.841 (369.35)	2.843 (369.11)	2.814 (369.76)	2.683 (370.12)
	1.1	2.822 (368.32)	2.843 (365.56)	2.843 (366.94)	2.814 (370.43)	2.681 (371.56)
	1.2	2.829 (368.21)	2.846 (367.68)	2.843 (365.86)	2.813 (370.22)	2.688 (368.55)
	1.3	2.832 (370.08)	2.850 (369.78)	2.843 (364.61)	2.812 (369.82)	2.694 (367.53)
	1.4	2.835 (370.58)	2.851 (371.70)	2.841 (367.16)	2.811 (371.78)	2.702 (369.98)
	1.5	2.841 (374.18)	2.850 (373.09)	2.842 (370.78)	2.810 (369.39)	2.714 (368.75)
15	0.1	2.808 (369.99)	2.809 (369.75)	2.809 (369.14)	2.810 (370.73)	2.810 (369.91)
	0.2	2.812 (370.98)	2.813 (370.39)	2.815 (369.89)	2.818 (371.08)	2.818 (369.97)
	0.3	2.819 (369.98)	2.823 (370.46)	2.828 (369.68)	2.827 (369.18)	2.823 (369.65)
	0.4	2.828 (370.74)	2.835 (370.93)	2.839 (370.26)	2.837 (370.72)	2.815 (369.02)
	0.5	2.837(370.49)	2.844 (370.79)	2.849 (370.87)	2.843 (370.41)	2.791 (370.46)
	0.6	2.850 (370.62)	2.851 (370.05)	2.856 (369.99)	2.844 (370.52)	2.761 (370.60)
	0.7	2.850 (370.61)	2.860 (369.40)	2.865 (370.84)	2.844 (370.36)	2.733 (370.02)
	0.8	2.853 (369.54)	2.868 (370.26)	2.866 (370.52)	2.835 (369.27)	2.709 (370.92)
	0.9	2.859 (369.53)	2.873 (369.72)	2.871 (370.32)	2.832 (369.81)	2.694 (370.56)
	EWMA 1.0	2.867 (370.51)	2.876 (370.10)	2.872 (370.83)	2.825 (369.29)	2.686 (369.11)
	1.1	2.875 (370.94)	2.878 (369.84)	2.869 (370.45)	2.823 (370.93)	2.680 (370.05)
	1.2	2.876 (369.14)	2.882 (370.09)	2.867 (369.41)	2.821 (370.96)	2.685 (370.68)
	1.3	2.880 (370.84)	2.883 (369.91)	2.867 (369.95)	2.821 (370.76)	2.693 (370.52)
	1.4	2.883 (370.50)	2.885 (370.16)	2.866 (370.05)	2.821 (370.88)	2.702 (369.55)
	1.5	2.886 (370.52)	2.885 (370.55)	2.867 (370.33)	2.823 (369.45)	2.715 (369.90)
20	0.1	2.864 (370.53)	2.864 (369.84)	2.864 (369.69)	2.864 (369.51)	2.864 (369.16
	0.2	2.866 (369.95)	2.867 (369.36)	2.867 (370.16)	2.869 (370.67)	2.870 (370.58)
	0.3	2.871 (370.22)	2.873 (369.58)	2.875 (370.16)	2.876 (370.43)	2.868 (369.79)
	0.4	2.876 (369.46)	2.877 (369.18)	2.880 (369.58)	2.878 (370.52)	2.848 (369.62)
	0.5	2.880 (370.06)	2.883 (370.87)	2.887 (370.83)	2.872 (369.18)	2.818 (369.04)
	0.6	2.885 (370.92)	2.890 (369.83)	2.889 (369.75)	2.868 (369.76)	2.781 (370.39)
	0.7	2.891 (370.14)	2.896 (370.03)	2.891 (370.03)	2.862 (370.17)	2.744 (370.43)
	0.8	2.894 (369.08)	2.899 (370.89)	2.889 (370.22)	2.857 (370.64)	2.724 (370.01)
	0.9	2.899 (369.96)	2.901 (370.31)	2.885 (370.48)	2.852 (370.44)	2.703 (370.21)
	EWMA 1.0	2.903 (370.11)	2.902 (370.87)	2.884 (369.90)	2.841 (369.85)	2.698 (369.76)
	1.1	2.905 (369.98)	2.903 (370.01)	2.885 (370.92)	2.835 (370.37)	2.695 (369.23)
	1.2	2.906 (370.39)	2.902 (370.04)	2.883 (370.06)	2.831 (369.61)	2.695 (370.46)
	1.3	2.906 (370.09)	2.903 (370.34)	2.881 (370.02)	2.830 (369.69)	2.703 (370.99)
	1.4	2.907 (369.50)	2.904 (369.70)	2.881 (370.48)	2.830 (370.06)	2.710 (370.66)
	1.5	2.907 (369.36)	2.904 (370.66)	2.880 (369.16)	2.833 (370.62)	2.723 (369.76)

(q, α, L) combination that provides the desired ARL performance. A detailed study on the optimal design for the GWMA-SR chart is out-of-scope for this paper and will be discussed in a future work;

iii. Comparing the line graphs in panels (a) and (b) with those in panels (c) and (d), it is easily observed that the attained ARL_0 is larger if L is larger; this is naturally expected since the control limits are wider for larger L which leads to a smaller probability of a signal.

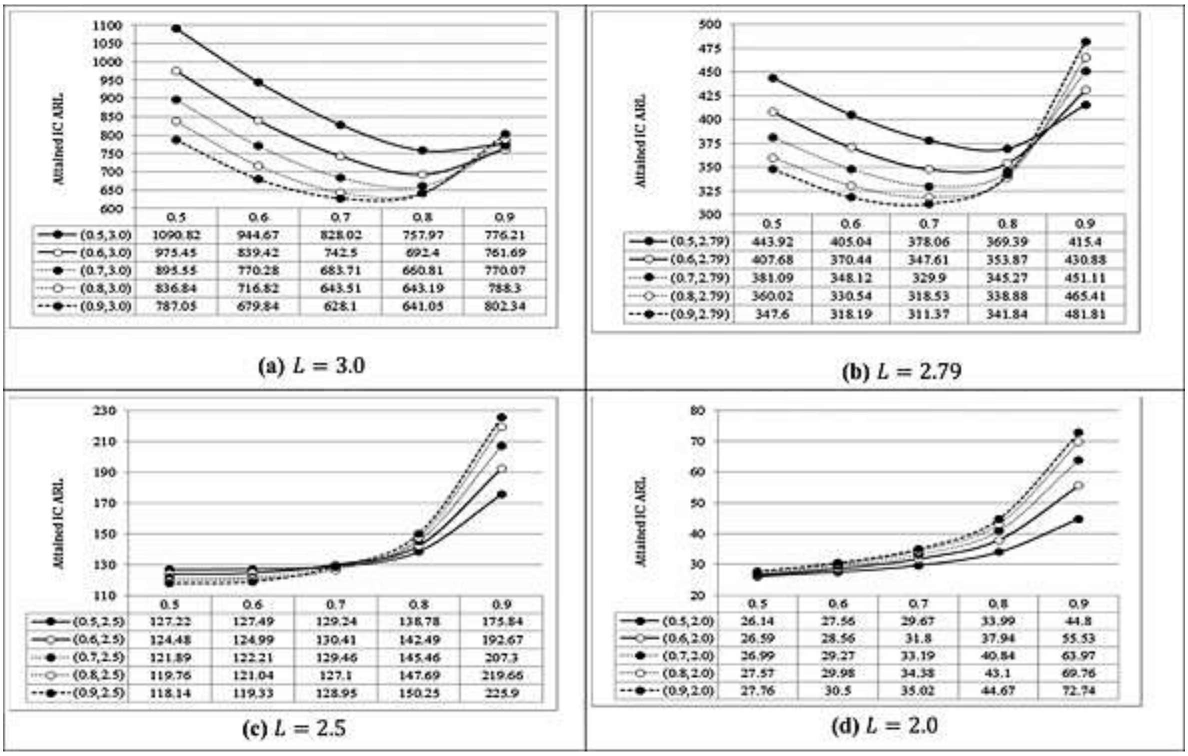

Figure 1. Attained ARL_0 versus q for different combinations of (α, L) when $n = 10$

Next, we study the performance of the GWMA-SR chart and compare it with some existing control charting procedures.

4. Performance study

The GWMA charts are generally more sensitive than the EWMA charts in detecting small shifts (see the results in Sheu and Lin[3], Lu[8] and Sheu and Yang[15]). In addition, Graham et al.[6] showed that in many cases the EWMA-SR chart outperforms the EWMA-SN chart (Graham et al.[7]) and the Shewhart-SR chart with run rules (Chakraborti and Eryilmaz[18]). Lu[8] further showed that the GWMA-SN chart is more sensitive than the parametric GWMA-$\overline{X}$ chart for normal and many non-normal distributions. Given the available results, it is of interest to compare the proposed GWMA-SR chart with the GWMA-$\overline{X}$ chart, the GWMA-SN chart and the EWMA-SR chart.

To study the performance of the GWMA-SR chart, we use some of the combinations of the parameters used in Table 1; these combinations ensure that the ARL_0 is close to 370. Because the underlying distribution is assumed to be symmetric, only the positive shifts (i.e. increases in the mean/median) are considered with magnitude δ = 0.05, 0.10, 0.25, 0.50, 0.75, 1.0 and 1.5; the results are equally applicable for negative or downward shifts. Also, as Shewhart-type charts are traditionally known to be efficient in detecting large shifts, we do not consider shifts more than 1.5; the purpose and focus of this article is only on detecting small shifts. The results of the comparison in performance of all the charts are displayed in Tables 2-4. We first compared the GWMA-SR chart with the EWMA-SR chart (which is regarded as the main competitor) and thereafter against the GWMA-SN and GWMA-$\overline{X}$ charts. A summary of the findings is as follows:

i. **GWMA-SR vs. EWMA-SR chart under normal distribution**

Table 2 shows the out-of-control (OOC) average run-length (ARL_1) values of the GWMA-SR and the EWMA-SR charts when n = 5 and 10 assuming that the underlying process can be modelled by the standard normal distribution. Both charts were designed so that their ARL_0's are close to 370.

The results show that for small shifts, i.e. when $\delta = 0.05$ and $\delta = 0.10$, the GWMA-SR chart performs better than the EWMA-SR chart (Graham et al.[6]) for a suitable combination of the parameters (q, α, L). For example, given a shift of $\delta = 0.05$ and sample size $n = 10$, the GWMA-SR chart with parameters ($q = 0.9$, $\alpha = 0.8$, $L = 2.698$) gives an $ARL_1 = 140.28$ while the EWMA-SR chart with parameters ($q = 0.9$, $L = 2.683$) gives an $ARL_1 = 151.79$. The GWMA-SR chart will therefore, on average, signal 11 samples sooner than the EWMA-SR chart. However, for larger shifts, the two charts perform similarly. For example, focussing on the results in Table 2 for $\delta = 1.5$ and $n = 10$, the GWMA-SR chart with parameters ($q = 0.5$, $\alpha = 1.2$, $L = 2.829$) gives an $ARL_1 = 2.01$ whilst the EWMA-SR chart with parameters ($q = 0.5$, $L = 2.815$) gives an $ARL_1 = 2.02$. Both charts are therefore expected to detect the shift on the second sample following the shift.

ii. **GWMA-SR vs. EWMA-SR charts under various non-normal distributions**

Table 3 shows the ARL_1 values of the GWMA-SR and the EWMA-SR charts when n = 10 under four non-normal symmetric (around zero) distributions. The distributions we considered have heavier or lighter tails than the normal distribution. We used the scaled Student's $\frac{t_\nu}{\sqrt{\nu/(\nu-2)}}$ distribution with degrees of freedom $\nu = 10$, the logistic$\left(0, \frac{\sqrt{3}}{\pi}\right)$ distribution, the uniform$(-\sqrt{3}, \sqrt{3})$ distribution and the Laplace$\left(0, \frac{1}{\sqrt{2}}\right)$ distribution. The parameters of these distributions were chosen so that the variance is 1 which makes the results comparable amongst different distributions. Note that the ARL_1 for the standard normal distribution (for n = 10) is included in the table for ease of comparison.

The results in Table 3 show that for small shifts, i.e. when $\delta = 0.05$ and $\delta = 0.10$, the GWMA-SR chart performs better than the EWMA-SR chart (Graham et al.[6]) for all the distributions considered. For example, for the logistic$\left(0, \frac{\sqrt{3}}{\pi}\right)$ distribution, the ARL_1 for the GWMA-SR chart is 52.78 while the ARL_1 for the for EWMA-SR chart is 58.78 when the shift is $\delta = 0.10$. These results confirm that the GWMA-SR chart outperforms the EWMA-SR chart for small shifts.

Table 2: Average run-lengths for the GWMA-SR and EWMA-SR charts for various shifts δ under the normal distribution when $ARL_0^* = 370$ and $n = 10$

δ	Chart	$n=5$				$n=10$			
		q	α	L	ARL_1	q	α	L	ARL_1
0.05	GWMA-SR	0.9	0.4	2.573	195.79	0.9	0.8	2.698	140.28
	EWMA-SR	0.9	1.0	2.666	243.68	0.9	1.0	2.683	151.79
0.10	GWMA-SR	0.9	0.6	2.657	93.35	0.9	0.7	2.718	58.75
	EWMA-SR	0.9	1.0	2.666	120.85	0.9	1.0	2.683	59.48
0.25	GWMA-SR	0.9	0.8	2.668	26.62	0.9	1.1	2.681	15.19
	EWMA-SR	0.9	1.0	2.666	26.96	0.9	1.0	2.683	15.42
0.50	GWMA-SR	0.9	1.3	2.679	9.80	0.9	1.5	2.714	5.72
	EWMA-SR	0.9	1.0	2.666	9.97	0.9	1.0	2.683	6.23
0.75	GWMA-SR	0.8	1.2	2.767	5.69	0.6	1.4	2.851	3.18
	EWMA-SR	0.8	1.0	2.768	5.81	0.6	1.0	2.841	3.26
1.00	GWMA-SR	0.5	1.1	2.657	4.06	0.5	1.5	2.841	2.31
	EWMA-SR	0.5	1.0	2.638	4.31	0.5	1.0	2.815	2.40
1.50	GWMA-SR	0.5	1.1	2.657	2.62	0.5	1.2	2.829	2.01
	EWMA-SR	0.5	1.0	2.638	3.19	0.5	1.0	2.815	2.02

Table 3: Average run-lengths for the GWMA-SR and EWMA-SR charts for various shifts δ under different symmetric distributions when $ARL_0^* = 370$ and $n = 10$

δ	Chart	q	α	L	normal(0,1)	t_{10}	logistic$\left(0,\frac{\sqrt{3}}{\pi}\right)$	uniform$(-\sqrt{3},\sqrt{3})$	Laplace$\left(0,\frac{1}{\sqrt{2}}\right)$
0.05	GWMA-SR	0.9	0.8	2.698	140.28	145.39	137.50	156.24	107.80
	EWMA-SR	0.9	1.0	2.683	151.79	168.29	157.88	179.78	126.46
0.10	GWMA-SR	0.9	0.8	2.698	58.94	54.99	52.78	63.84	39.40
	EWMA-SR	0.9	1.0	2.683	59.48	61.24	58.78	72.30	42.69
0.50	GWMA-SR	0.9	1.5	2.714	5.72	5.44	5.34	6.37	4.83
	EWMA-SR	0.9	1.0	2.683	6.23	5.93	5.81	6.87	5.25
1.00	GWMA-SR	0.5	1.5	2.841	2.31	2.27	2.27	2.48	2.25
	EWMA-SR	0.5	1.0	2.815	2.40	2.37	2.36	2.57	2.33

Table 4: Average run-lengths for the GWMA-SR, GWMA-SN and GWMA- $\bar{X}$ charts for various shifts δ when $ARL_0^* = 370$ and $n = 10$ under different symmetric distributions

δ	Chart	q	α	L	normal(0,1)	t_{10}	logistic$\left(0,\frac{\sqrt{3}}{\pi}\right)$	uniform$(-\sqrt{3},\sqrt{3})$	Laplace$\left(0,\frac{1}{\sqrt{2}}\right)$
0.00	GWMA-SR	0.9	0.9	2.687	370.88	371.01	370.90	370.05	371.75
	GWMA-SN	0.9	0.9	2.695	370.24	370.69	368.68	369.07	370.85
	GWMA- $\bar{X}$	0.9	0.9	2.720	369.41	370.74	362.74	382.22	355.36
0.05	GWMA-SR	0.9	0.9	2.687	150.01	155.67	147.27	167.72	115.28
	GWMA-SN	0.9	0.9	2.695	195.63	178.24	169.60	246.48	101.34
	GWMA- $\bar{X}$	0.9	0.9	2.720	156.22	159.82	155.03	155.60	154.14
0.10	GWMA-SR	0.9	0.9	2.687	62.01	56.69	55.54	67.16	40.90
	GWMA-SN	0.9	0.9	2.695	81.23	70.48	66.57	126.61	36.72
	GWMA- $\bar{X}$	0.9	0.9	2.720	57.92	57.30	58.39	58.48	57.82
0.25	GWMA-SR	0.9	0.9	2.687	15.21	14.01	13.67	16.72	11.10
	GWMA-SN	0.9	0.9	2.695	19.34	16.97	16.17	31.63	10.71
	GWMA- $\bar{X}$	0.9	0.9	2.720	13.86	13.80	13.79	13.83	13.88
0.50	GWMA-SR	0.9	0.9	2.687	6.44	6.04	5.91	7.03	5.31
	GWMA-SN	0.9	0.9	2.695	7.59	6.94	6.66	11.17	5.31
	GWMA- $\bar{X}$	0.9	0.9	2.720	5.57	5.56	5.52	5.53	5.51
1.00	GWMA-SR	0.9	0.9	2.687	3.42	3.42	3.39	3.64	3.35
	GWMA-SN	0.9	0.9	2.695	3.74	3.56	3.50	4.54	3.30
	GWMA- $\bar{X}$	0.9	0.9	2.720	2.56	2.55	2.55	2.55	2.56

iii. **GWMA-SR vs. GWMA-SN and GWMA-$\bar{X}$ under various distributions**

To compare the GWMA-SR chart with the GWMA-SN and GWMA-$\bar{X}$ charts, we used the same symmetric distributions (with the same parameters) as in the preceding section; this includes the standard normal distribution too. The corresponding results are displayed in Table 4 for n = 10 when the attained ARL_0 is close to 370.

From the results in Table 4, it can be observed that the GWMA-$\bar{X}$ chart outperforms both the GWMA-SR and GWMA-SN charts (for shifts $\delta \geq 0.1$) when the underlying distribution is the standard normal or the scaled Student's t_{10} distribution. This result is not unexpected since the GWMA-$\bar{X}$ chart is specifically designed for the normal distribution and, the scaled Student's t_{10} distribution does not deviate much from the normal distribution. However, it is important to note the following points:

a) While the attained ARL_0 values of the GWMA-SR and GWMA-SN charts remain unchanged for different underlying distributions, the attained ARL_0 of the GWMA-$\bar{X}$ fluctuates. For instance, the GWMA-$\bar{X}$ chart with $q = 0.9$, $\alpha = 0.9$, $L = 2.720$ has an $ARL_0 = 369.41$ under normality, but it has an $ARL_0 = 382.22$ under the uniform$(-\sqrt{3}, \sqrt{3})$ distribution. This non-robustness of the GWMA-$\bar{X}$ chart occurs because the GWMA-$\bar{X}$ is a parametric chart designed for a specific distribution. In cases where normality is in question or cannot be verified, the GWMA-SR chart and the GWMA-SN can be valuable alternatives;

b) The GWMA-SR chart generally outperforms the GWMA-SN chart for all shifts in case of the scaled Student's t_{10} distribution, the logistic$\left(0, \frac{\sqrt{3}}{\pi}\right)$ distribution and the uniform$(-\sqrt{3}, \sqrt{3})$ distribution. For example, the ARL_1's are 155.67 vs. 178.24, 147.27 vs. 169.60 and 167.72 vs. 246.48, respectively, for $\delta = 0.05$. Even for a shift of size $\delta = 1.00$, the ARL_1's are 3.42 vs. 3.56, 3.39 vs. 3.50 and 3.64 vs. 4.54;

c) In case of the Laplace$\left(0, \frac{1}{\sqrt{2}}\right)$ distribution, the GWMA-SN outperforms the GWMA-SR for shifts $\delta = 0.05$, 0.10 and 0.25; the ARL_1's are 101.34 vs. 115.28, 36.72 vs. 40.90 and 10.71 vs. 11.10, respectively. For shifts $\delta = 0.50$ and 1.00, the performance of the charts is similar;

d) The GWMA-$\bar{X}$ chart performs marginally better than the GWMA-SR and GWMA-SN charts for a shift of $\delta = 1.00$ under the logistic$\left(0, \frac{\sqrt{3}}{\pi}\right)$, uniform$(-\sqrt{3}, \sqrt{3})$ and Laplace$\left(0, \frac{1}{\sqrt{2}}\right)$ distribution.

As a general recommendation for the implementation of the GWMA-SR chart is that value of q such as 0.8 or 0.9 and values of α in the region 0.4 to 0.9 should be useful in detecting a shift of $\delta < 0.5$ while $q < 0.8$ and $\alpha > 1$ should be useful in detecting larger shifts. In the next section, an example is provided to illustrate the proposed GWMA-SR chart.

5. Example

To demonstrate the application and performance of the proposed GWMA-SR chart against the GWMA-SN chart, we draw 15 random samples each of size $n = 10$ from a normal distribution with mean 0.25 and variance 1.00. If we assume the true mean/median of the process is 0.00, the simulated data can be viewed as observations from an out-of-control (OOC) process following a shift of 0.25 standard deviation in the location.

Setting the parameters of the GWMA-SR chart equal to $q = 0.9$, $\alpha = 0.9$ and $L = 2.687$, the control limits and centerline are calculated using equation (8) to be $UCL =$ 10.90, $LCL =$ –10.90 and $CL = 0$, respectively. For this choice of the parameters, the attained ARL_0 is 370.88 and obtained from Table 1 or Table 4.

The parameters for the GWMA-SN chart were taken to be $q = 0.9$, $\alpha = 0.9$ and $L = 2.695$. The control limits and centerline are calculated to be $UCL = 5.881$, $LCL = 4.119$ and $CL = 5$, respectively. The attained ARL_0 of the GWMA-SN chart is 370.24, which is shown in Table 5. As the attained ARL_0 values are approximately equal, the two charts are at an equal footing in terms of their in-control performance.

The two control charts are shown in Figure 2; from panels (a) and (b), we observe the following:

i. Although the general trend in the charting statistics is similar, the GWMA-SR chart detects the shift and signals on the 9th observation (i.e. the run-length is 9) whereas the GWMA-SN chart does not detect the shift and does not signal;
ii. Both the GWMA-SR and the GWMA-SN charts use steady-state control limits;
iii. The centerline of the GWMA-SR chart is equal to zero (which makes it easy to visually distinguish between an upward/positive shift and a downward/negative shift), whereas the centerline of the GWMA-SN chart is equal to 5;
iv. Neither of the two charts' vertical axes is in the original scale of measurement. This happens since the two charts do not use the original numerical measurements, i.e. the GWMA-SR chart's key building block is the Wilcoxon signed-rank statistic (which is based on counting and ranking the observations within the samples) and the GWMA-SN chart's basic building block is the well-known sign test (which is based on counting only). Although this can be seen as a shortcoming, the fact these charts are distribution-free far outweighs this inconvenience.

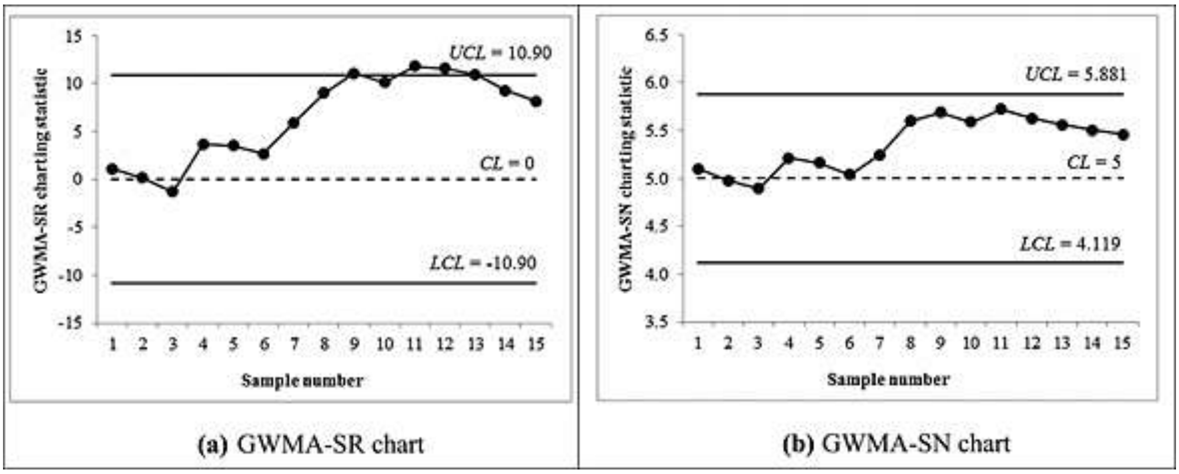

(a) GWMA-SR chart (b) GWMA-SN chart

Figure 2. **The GWMA-SR and GWMA-SN charts**

6. Concluding remarks

A new distribution-free GWMA chart to detect small sustained upward or downward steps shifts in the location has been proposed based on the Wilcoxon signed-rank statistic; the proposed chart extends the existing EWMA-SR and GWMA-SN charts for a known in-control value of the process median. An advantage of the GWMA class of charts (over the EWMA charts) lies in the additional parameter α which provides more flexibility in its design and better detection ability for small shifts. For a specified ARL_0 of 370 and different combinations of the parameters (q, α), the charting constant $L > 0$ has been obtained which will assist in the design and implementation of the chart. The performance of the GWMA-SR chart has been evaluated by means of simulation. It has been found that the GWMA-SR chart (with suitable parameters) performs better than the GWMA-SN and the EWMA-SR charts. Because both the GWMA-SN and the EWMA-SR charts are well-known to be better than many parametric and nonparametric control charts, the GWMA-SR chart should be a useful addition to the quality practitioner's collection of control charts to choose from. It will be of interest to consider the problem when the population median (for which the control chart is built) is not specified; this will be pursued in future work.

Acknowledgements

Research of the first author was supported in part by STATOMET at the University of Pretoria, South Africa and National Research Foundation through the SARChI Chair at the University of Pretoria, South Africa.

References:

1. Roberts SW. Control chart tests based on geometric moving averages. *Technometrics* 1959; **1**(3):239-250.

2. Ruggeri F, Kenett RS, Faltin FW. Exponentially weighted moving average (EWMA) control chart. In *Encyclopedia of Statistics in Quality and Reliability,* vol. 2. John Wiley & Sons: Hoboken, New Jersey, 2007; 633-639.

3. Sheu SH, Lin TC. The generally weighted moving average control chart for detecting small shifts in the process mean. *Quality Engineering* 2003; **16**(2):209-231.

4. Chakraborti S, Human SW, Graham MA. Nonparametric (distribution-free) quality control charts. In *Handbook of Methods and Applications of Statistics: Engineering, Quality Control, and Physical Sciences*, Balakrishnan N (ed). John Wiley & Sons: Hoboken, New Jersey, 2011; 298–329.

5. Amin RW, Searcy AJ. A nonparametric exponentially weighted moving average control scheme. *Communications in Statistics-Simulation and Computation* 1991; **20**(4):1049-1072.

6. Graham MA, Chakraborti S, Human SW. A nonparametric exponentially weighted moving average signed-rank chart for monitoring location. *Computational Statistics & Data Analysis* 2011; **55**(8):2490-2503.

7. Graham MA, Chakraborti S, Human SW. A nonparametric EWMA sign chart for location based on individual measurements. *Quality Engineering* 2011; **23**(3):227-241.

8. Lu SL. An Extended Nonparametric Exponentially Weighted Moving Average Sign Control Chart. *Quality and Reliability Engineering International* 2015; **31**(1):3-13.

9. Konijn HS. Symmetry tests. In *Encyclopedia of Statistical Sciences* (2nd ed.), vol. 13. John Wiley & Sons: Hoboken, New Jersey, 2006; 8507-8510.

10. Gibbons JD, Chakraborti S. *Nonparametric Statistical Inference*, 5th ed. Taylor and Francis: Boca Raton, FL, 2003.

11. Nakagawa T, Osaki S. The discrete Weibull distribution. *IEEE Transactions on Reliability* 1975; **5**:300-301.

12. Montgomery DC. *Statistical Quality Control: A Modern Introduction*, 7th ed. John Wiley & Sons: Hoboken, New Jersey, 2013.

13. Lucas JM, Saccucci MS. Exponentially weighted moving average control schemes: properties and enhancements. *Technometrics* 1990; **32**(1):1-2.

14. Human SW, Graham MA. Average run-lengths and operating characteristic curves. In *Encyclopedia of Statistics in Quality and Reliability,* vol. 1. John Wiley & Sons: Hoboken, New Jersey, 2007; 159-168.

15. Sheu SH, Yang L. The generally weighted moving average control chart for monitoring the process median. *Quality engineering* 2006; **18**(3):333-344.

16. Teh SY, Khoo MB, Wu Z. Monitoring process mean and variance with a single generally weighted moving average chart. *Communications in Statistics-Theory and Methods* 2012; **41**(12):2221-2241.

17. Sheu SH, Huang CJ, Hsu TS. Maximum chi-square generally weighted moving average control chart for monitoring process mean and variability. *Communications in Statistics-Theory and Methods* 2013; **42**(23):4323-4341.

18. Chakraborti S, Eryilmaz S. A nonparametric Shewhart-type signed-rank control chart based on runs. *Communications in Statistics—Simulation and Computation* 2007; **36**(2):335-356.

Appendix

A1. Convergence of $\lim_{t\to\infty} \boldsymbol{Q_t} = \sum_{i=1}^{\infty}\left(\boldsymbol{q}^{(i-1)^{\alpha}} - \boldsymbol{q}^{i^{\alpha}}\right)^2$ for $0 \leq \boldsymbol{q} < 1, \boldsymbol{\alpha} > 0$

We have $Q_t = \sum_{i=1}^{t}\left(q^{(i-1)^{\alpha}} - q^{i^{\alpha}}\right)^2 = \sum_{i=1}^{t} q^{2(i-1)^{\alpha}} + \sum_{i=1}^{t} q^{2i^{\alpha}} - 2\sum_{i=1}^{t} q^{(i-1)^{\alpha}} q^{i^{\alpha}}$. We consider two scenarios:

i. For $q = 0$, $\lim_{t\to\infty} Q_t = \sum_{i=1}^{\infty}\left(q^{(i-1)^{\alpha}} - q^{i^{\alpha}}\right)^2 = 1$;

ii. For $0 < q < 1$, we have $q^{(i-1)^{\alpha}} > q^{i^{\alpha}} \Rightarrow q^{(i-1)^{\alpha}} q^{i^{\alpha}} > q^{2i^{\alpha}}$. Substituting $q^{(i-1)^{\alpha}} q^{i^{\alpha}}$ by $q^{2i^{\alpha}}$, it follows that $Q_t < \left(\sum_{i=1}^{t} q^{2(i-1)^{\alpha}} + \sum_{i=1}^{t} q^{2i^{\alpha}} - 2\sum_{i=1}^{t} q^{2i^{\alpha}}\right) = \left(\sum_{i=1}^{t} q^{2(i-1)^{\alpha}} - \sum_{i=1}^{t} q^{2i^{\alpha}}\right)$. It then follows that $Q_t < \left(1 - q^{2t^{\alpha}}\right) < 1$.

So, for $0 < q < 1$, the monotonically increasing sequence $\{Q_t; t = 1,2,3, \ldots\}$ is bounded above and is therefore convergent. Further, $0 < Q_t < 1$ for all values of t; this implies that $0 < \lim_{t\to\infty} Q_t < 1$ and so there exists a number (denoted by Q) in the interval (0,1) such that $\lim_{t\to\infty} Q_t = Q$ for $0 < q < 1$. This completes the proof.

A2. For $\boldsymbol{r} = \mathbf{2}, \mathbf{3}, \mathbf{4}, \ldots$, $\mathbf{Pr}[\boldsymbol{R} = \boldsymbol{r}] = \boldsymbol{I_{r-1}} - \boldsymbol{I_r}$, where $\boldsymbol{I_r} = \mathbf{Pr}[\cap_{i=1}^{r} \boldsymbol{A_i^c}]$

$\Pr[R = r] = \Pr\left[\left\{\cap_{i=1}^{r-1} A_i^c\right\} \cap \mathrm{A_r}\right] = \Pr\left[\cap_{i=1}^{r-1} A_i^c\right] - \Pr\left[\left\{\cap_{i=1}^{r-1} A_i^c\right\} \cap A_i^c\right] = \Pr\left[\cap_{i=1}^{r-1} A_i^c\right] - \Pr[\cap_{i=1}^{r} A_i^c]$.

Therefore, $\Pr[R = r] = I_{r-1} - I_r$, where $I_r = \Pr[\cap_{i=1}^{r} A_i^c]$.

A3. $\boldsymbol{ARL} = \mathbf{1} + \sum_{r=1}^{\infty} \boldsymbol{I}_{\mathrm{r}}$

Because $\Pr[R = r] = I_{\mathrm{r}-1} - I_{\mathrm{r}}$, we have $ARL = \sum_{r=1}^{\infty} r \Pr[R = r]$. By expanding and re-arranging some of the terms, we obtain

$ARL = \Pr[R = 1] + \sum_{r=2}^{\infty} r \Pr[R = r] = 1 - \Pr[A_1^c] + \sum_{r=2}^{\infty} r(I_{\mathrm{r}-1} - I_{\mathrm{r}}) = 1 - \Pr[A_1^c] + I_1 + \sum_{r=1}^{\infty} I_{\mathrm{r}} = 1 + \sum_{r=1}^{\infty} I_{\mathrm{r}}$,

as required.

Biographies

N. Chakraborty has an MSc from the Department of Statistics at the University of Pune, India. He is currently a PhD student at the University of Pretoria, South Africa. Presently, his main area of research interest is statistical process control.

S. Chakraborti is a professor of Statistics in the University of Alabama in Tuscaloosa, AL, USA. His research interests include the theory and application of nonparametric and robust statistical methodologies with emphasis on statistical process control. Professor Chakraborti is a fellow of the American Statistical Association and an elected member of the International Statistical Institute. He is the author and co-author of many publications including the co-authored book Nonparametric Statistical Inference, 5th edition, published by Taylor and Francis.

S.W. Human has obtained his PhD in Mathematical Statistics from the University of Pretoria, South Africa. Dr Human has authored/co-authored numerous peer-reviewed journal articles and has presented his research at several national and international conferences. He also serves as a reviewer for a number of reputed international statistical journals. He is a member of the American Statistical Association and the South African Statistical Association. His main areas of research include statistical quality control and distribution theory.

N. Balakrishnan is a distinguished university professor in the Department of Mathematics and Statistics at McMaster University, Hamilton, Ontario, Canada. He is a fellow of the American Statistical Association, a fellow of the Institute of Mathematical Statistics and an elected member of the International Statistical Institute. His research interests are quite wide covering a range of topics including ordered data analysis, distribution theory, quality control, reliability, survival analysis and robust inference. He is currently the editor-in-chief of Communications in Statistics and the Encyclopedia of Statistical Sciences.